Wearable Sweat Rate Sensors

Murat A. Yokus[1], Talha Agcayazi[1], Matt Traenkle[2], Alper Bozkurt[1] and Michael A. Daniele[1,2]
[1]Department of Electrical and Computer Engineering
[2]Joint Department of Biomedical Engineering
North Carolina State University and University of North Carolina at Chapel Hill
Raleigh, NC USA
mdaniel6@ncsu.edu

***Abstract*—Sweat plays a significant role in human homeostasis by regulating the body temperature via evaporative cooling under heat or work stress. Water and electrolytes (mainly sodium and chloride) constitute almost 99% of the sweat composition. Excessive sweat loss disturbs the human homeostasis, impairs circulation, and impedes heat dissipation. Some of the limitations of the conventional sweat loss measurement techniques lie in their wearability, sweat sampling, analyte contamination from skin, and evaporation. To overcome these limitations, we have developed a wearable sensor for continuous sweat rate measurement in wearable form factors. The wearable sensor consists of low-cost printed interdigitated electrodes for impedance sensing, a serpentine shaped paper-based microfluidic channel, and a polyurethane encapsulation layer. In this report, we present the benchtop characterization of the proposed sensor's capability to track the sweat rate. The microfluidics can hold sweat volumes up to 82 µL and enable the detection of sweat rates on various locations of the body for extended periods.**

Keywords—Impedance sensing; paper microfluidics; sweat rate; wearable; admittance

I. INTRODUCTION

Sweating occurs due to the activation of eccrine glands by temperature, emotion, stress, gustation, or medical illnesses [1]. Elevated body temperature is the primary cause of sweat generation, which holds a vital role in thermoregulation of the body [2]. The eccrine glands are widely distributed across the body (1.6 to 4 million) and show a regional density variation, with the highest gland density on volar surfaces of fingers (530 glands cm^{-2}) [3, 4]. Taking into account the spreading and density of the sweat glands, a prolonged workout in extreme climatic conditions may cause whole-body sweat loss as much as 16 L or 20 nL min^{-1} $gland^{-1}$ [3, 5]. The body cannot sustain the high sweating rates for extended periods as it may cause loss of essential electrolytes (*e.g.*, sodium and chloride), which are necessary for maintaining homeostasis within the body. For instance, during an exercise, failing to restore the fluid-need will increase the chances of dehydration which may lead to elevation of core body temperature and heart rate, hypertonicity of body fluids as well as impairment of blood flow [6]. Exercise-induced dehydration may lead to life-threatening conditions such as heat stroke, rhabdomyolysis, muscle cramps, hypernatremia, as well as a decrease in mental and cognitive performance [7]. Thus, tracking real-time sweat rate values would enable users or athletes to achieve their optimum performance and obviate the potential health complications.

This work was supported by the U.S. National Science Foundation through Nanosystems Engineering Research Center for Advanced Self-Powered Systems of Integrated Sensors and Technologies (ASSIST) under Grant EEC 1160483.

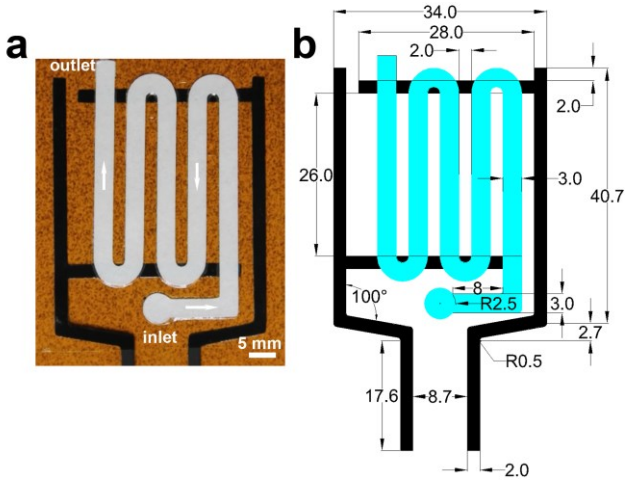

Fig. 1. a) A picture of fabricated sweat rate sensor, consisting of printed carbon interdigitated electrodes, a paper-based microfluidic layer, and a transparent and waterproof polyurethane encapsulation layer. **b)** Schematic of the fabricated sensors. Unit: mm.

Conventional measurements of sweat rate or total sweat loss include the whole-body wash-down technique and sweat collection with plastic bags, absorbent patches, and Macroduct [8]. These methods are carried out in controlled lab settings, require complicated steps and trainers, and are sensitive to analyte degradation and skin contamination. Untraditional sweat rate monitoring methods have also been developed, measuring impedance, optical reflectance, perfused sweat volume, or water vapor in a microfluidic channel, swellable hydrogel, epidermal microfluidic device, or in a sealed chamber, respectively [9-13]. These methods enable continuous sampling and real-time analysis of sweat loss with minimal sweat evaporation.

Herein, we demonstrate a printed impedance sensor with integrated paper-based microfluidics for sweat rate monitoring (Fig. 1). The novelty of this study lies in the integration of paper-based microfluidics with inexpensive printed electronics for sweat rate assessment. This study is an improved and low-cost version of our previous work on interdigitated impedance-based sweat rate sensing [14]. The proposed work incorporates paper-based microfluidics because of their low-cost, ease of fabrication, and continuous fluid wicking properties [15]. Their

978-1-7281-6801-2/20/$31.00 ©2020 IEEE

PDMS counterparts require sophisticated microfabrication techniques, hydrophilic microchannels, as well as optimization of channel dimensions for attaining optimum bursting pressures [16]. The sensor utilizes a similar impedance sensing approach that was presented in [10, 17]. The printed sensors were coupled with a paper-based microfluidic channel for extended fluid collection, which would enable continuous sweat draw and sweat loss assessment when interfaced with the skin.

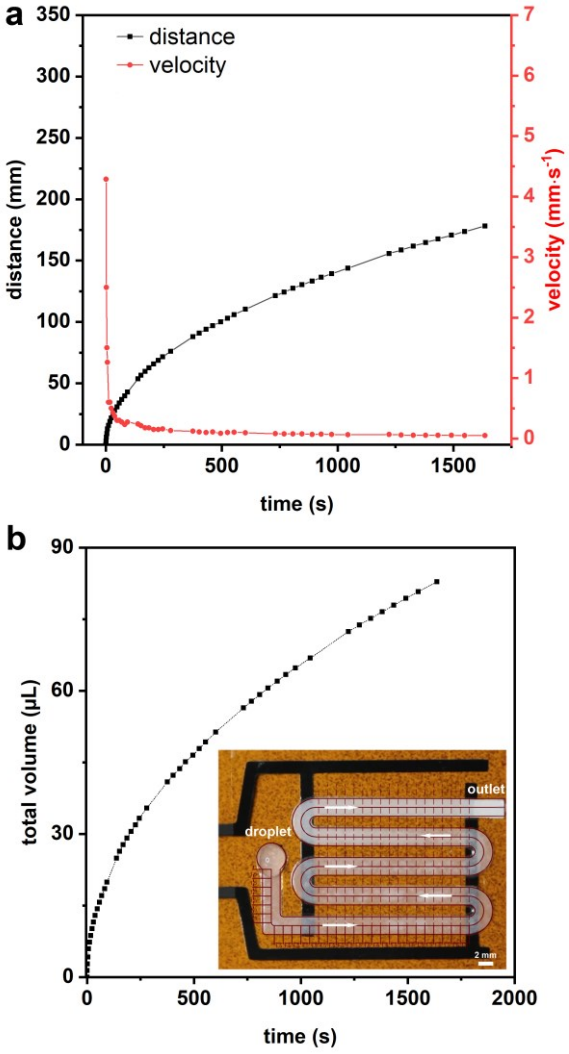

Fig. 2. a) Fluid velocity and distance travelled by the fluid over the course of testing. **b)** Filling of the microfluidic channel as a function of time. Inset: Sweat rate sensor with 1X PBS filled microfluidic channel.

II. Materials and Methods

A. Materials

The used materials include Whatman filter paper (Grade 541, thickness: 155 µm, VWR LLC, USA); phosphate buffer saline (1X PBS); carbon paste (C2050106P7, Gwent Ltd, UK); TegaDerm™ (3M Co., USA).

B. Fabrication of Sweat Rate Sensors

We designed the sweat rate sensor with interdigitated electrodes in AutoCAD and fabricated by screen printing carbon ink on a 50 µm thick polyimide film using a 230 mesh size frame (Fig. 1b). We cured the printed sensor at 80°C for 15 min. A serpentine-shaped paper channel with a 3 mm channel width was cut from a 155 µm thick filter paper using Silhouette Cutter. The microfluidic paper channel was placed onto the printed electrodes and encapsulated with a polyurethane Tegaderm layer. We created an inlet opening with ~20 mm^2 on the encapsulation layer. We then made an outlet opening with 14 mm^2 on the polyimide layer facing the backside of the sensor to ensure continuous fluid flow.

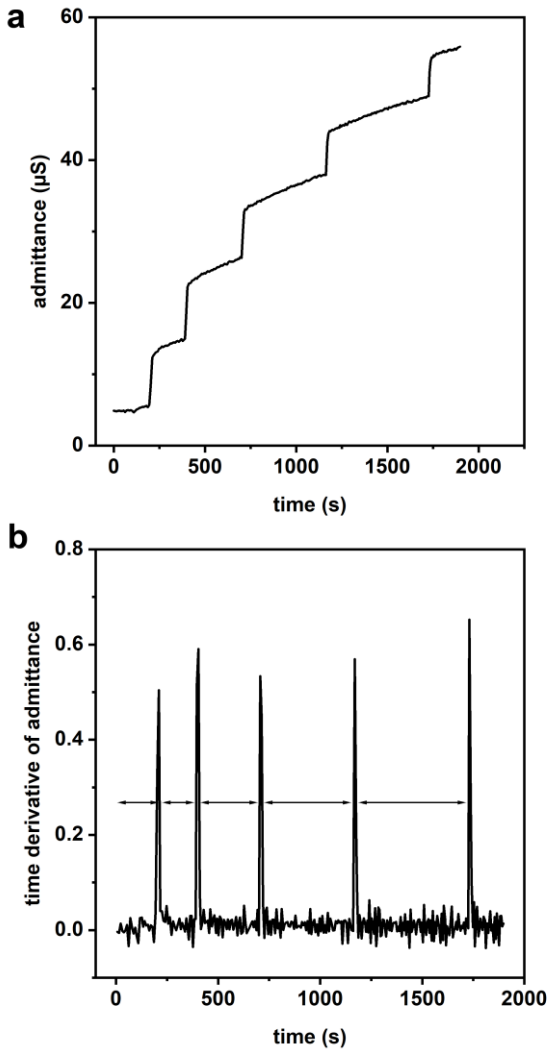

Fig. 3. a) Admittance change of the sweat rate sensor as 1X PBS solution travels throughout the paper microfluidic channel and crosses subsequent electrode fingers. Crossing a new electrode results in a jump in admittance. **b)** Time derivation of the admittance data in (a). The distinct peaks correspond to the admittance steps in (a).

C. Microfluidic and Electrical Characterization

We used 200 µL of 1X PBS solution as an artificial sweat solution and drop-cased to the inlet of the microfluidic channel for microfluidic characterization of the paper-based channel. The fluid flow was recorded continuously using a digital camera. We measured the electrical impedance between the interdigitated electrodes simultaneously using a Gamry reference 600+ potentiostat. The recorded video was used for calculation of the fluid velocity and time-dependent filling of the

paper-based channel. We used Electrochemical Impedance Spectroscopy (EIS) (100 kHz, V_{AC} = 10 mV, and V_{dc} = 0 V) for measuring the impedance between the electrodes as the fluid slowly filled the microfluidic channel.

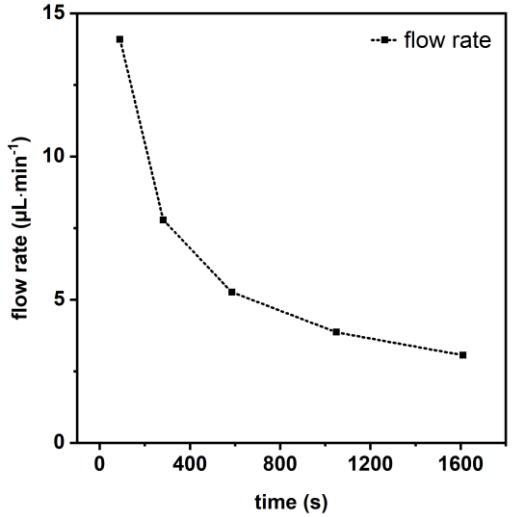

Fig. 4. Demonstration of a continuous flow rate measurement. The flow rate will be altered based on the perspiration rate on the skin surface.

III. Results and Discussions

The fabricated sweat rate sensor was shown in Fig. 1a. It is a printed and flexible sensor offering a low-cost approach for continuous quantification of the sweat rate or sweat loss. The sensor consists of three layers: a flexible polyimide film with printed interdigitated electrodes, a paper-based microfluidic channel for collection and continuous transport of the fluid, and a polyurethane cover layer for encapsulation of the microfluidic channel to prevent fluid evaporation.

The capillary pressure-driven transport of 1X PBS solution across the paper microfluidic channel is shown in Fig. 2a. The distance traveled by the fluid in a porous media slowed down over time because of a decrease in fluid velocity. As the fluid is transported throughout the paper microfluidic channel, the capillary pressure decreases, leading to a decrease in the fluid velocity, according to Darcy's law [18]. Because of the square root dependence of the distance (*i.e.*, visible wetted front of the paper) to time (t) (Lucas-Washburn equation), the distance taken by the fluid slows down over time [19]. Overall, the paper-based microfluidic channel can hold 82 μL of fluid in approx. 30 min fill time, corresponding to approx. 15 μL of fluid collection per the microfluidic channel length between each electrode fingers (Fig. 2b).

In addition to the fluid volume per serpentine line, real-time monitoring of sweat rate also requires the assessment of the time points at which the fluid crosses the fingers of the interdigitated electrodes. This was achieved by monitoring the admittance between the electrode fingers as the fluid traveled on the serpentine-shaped microfluidic channel. When the fluid crossed a new electrode pair, a sharp increase in the admittance plot was observed (Fig. 3a). The step size in the admittance curve is dependent on the conductivity of the solution and the contact area between the paper microfluidic channel and the printed electrodes. Fig. 3b shows the time derivation of the admittance plot in Fig. 3a. The location of the distinct peaks corresponds to the increase in admittance whenever the fluid passes an electrode pair. The time interval between each peak extended over time, which was attributed to the decrease in fluid velocity as the fluid got closer to the outlet of the microfluidic channel. The flow rate was calculated using the volume of fluid collection per serpentine line and the locations (time points) of the admittance peaks (Fig. 4). When the sweat rate sensor is worn on the skin surface, the flow rate graph would be modified in line with the rate of perspiration on the skin surface. Considering the maximum sweat rate as 20 $nL \cdot min^{-1} \cdot gland^{-1}$, average sweat gland density as 150 $glands \cdot cm^{-2}$, and ~0.2 cm^2 inlet area, the sweat generation per this area would be 0.6 $\mu L \cdot min^{-1}$. This number indicates that the starting flow rate of the fabricated sensor will not be a limiting factor for continuous wicking of the perspired sweat on the skin surface for real-time sweat rate assessment. At this flow rate, the total time required to fill out the microfluidic paper channel (82 μL) would be over 2 hours. Further modifications to the inlet area and the width of the microfluidic channel can be made for the collection of increased sweat volumes.

IV. Conclusion and Future Work

In this study, we demonstrate the *in vitro* operation of an inexpensive and flexible patch for continuous sweat rate monitoring. Facile integration of a paper-based microfluidic channel with printed interdigitated electrodes provides a passive sweat transport platform for prolonged sweat rate monitoring. The integration of this sensor with other biochemical sensors will enable real-time sweat analysis and the correlation of sweat-rate dependent biomarkers. Future work will involve *in situ* testing of the proposed sensor when the human subjects undergo active exercise conditions.

REFERENCES

[1] T. Schlereth, Dieterich, and Birklein, "Hyperhidrosis-Causes and Treatment of Enhanced Sweating," *Deutsches Arzteblatt International,* vol. 106, pp. 32-Ii, Jan 16 2009.

[2] E. R. Nadel, R. W. Bullard, and J. A. Stolwijk, "Importance of skin temperature in the regulation of sweating," *J Appl Physiol,* vol. 31, pp. 80-7, Jul 1971.

[3] N. A. S. Taylor and C. A. Machado-Moreira, "Regional variations in transepidermal water loss, eccrine sweat gland density, sweat secretion rates and electrolyte composition in resting and exercising humans," *Extreme Physiology & Medicine,* vol. 2, pp. 4-4, 2013.

[4] K. Sato, W. H. Kang, K. Saga, and K. T. Sato, "Biology of Sweat Glands and Their Disorders .1. Normal Sweat Gland-Function," *Journal of the American Academy of Dermatology,* vol. 20, pp. 537-563, Apr 1989.

[5] K. Sato and F. Sato, "Individual Variations in Structure and Function of Human Eccrine Sweat Gland," *American Journal of Physiology,* vol. 245, pp. R203-R208, 1983.

[6] V. A. Convertino, L. E. Armstrong, E. F. Coyle, G. W. Mack, M. N. Sawka, L. C. Senay*, et al.*, "American College of Sports Medicine position stand - Exercise and fluid replacement," *Medicine and Science in Sports and Exercise,* vol. 28, pp. R1-R7, Jan 1996.

[7] M. N. Sawka, L. M. Burke, E. R. Eichner, R. J. Maughan, S. J. Montain, and N. S. Stachenfeld, "Exercise and fluid replacement," *Medicine and Science in Sports and Exercise,* vol. 39, pp. 377-390, Feb 2007.

[8] C. H. Liu, T. L. Xu, D. D. Wang, and X. J. Zhang, "The role of sampling in wearable sweat sensors," *Talanta,* vol. 212, May 15 2020.

[9] F. J. Zhao, M. Bonmarin, Z. C. Chen, M. Larson, D. Fay, D. Runnoe*, et al.*, "Ultra-simple wearable local sweat volume monitoring patch based on swellable hydrogels," *Lab on a Chip,* vol. 20, pp. 168-174, Jan 7 2020.

[10] S. B. Kim, K. Lee, M. S. Raj, B. Lee, J. T. Reeder, J. Koo*, et al.*, "Soft, Skin-Interfaced Microfluidic Systems with Wireless, Battery-Free Electronics for Digital, Real-Time Tracking of Sweat Loss and Electrolyte Composition," *Small,* vol. 14, Nov 8 2018.

[11] P. Salvo, A. Pingitore, A. Barbini, and F. Di Francesco, "A wearable sweat rate sensor to monitor the athletes' performance during training," *Science & Sports,* vol. 33, pp. e51-e58, 2018/04/01/ 2018.

[12] J. T. Reeder, J. Choi, Y. G. Xue, P. Gutruf, J. Hanson, M. Liu*, et al.*, "Waterproof, electronics-enabled, epidermal microfluidic devices for sweat collection, biomarker analysis, and thermography in aquatic settings," *Science Advances,* vol. 5, Jan 2019.

[13] V. Jain, M. Ochoa, H. J. Jiang, R. Rahimi, and B. Ziaie, "A mass-customizable dermal patch with discrete colorimetric indicators for personalized sweat rate quantification," *Microsystems & Nanoengineering,* vol. 5, Jun 17 2019.

[14] M. A. Yokus, C. Hass, T. Agcayazi, A. Bozkurt, and M. A. Daniele, "Towards a Wearable Perspiration Sensor," *2017 Ieee Sensors,* pp. 1260-1262, 2017.

[15] M. A. Yokus, T. Saha, J. Fang, M. D. Dickey, O. D. Velev, and M. A. Daniele, "Towards Wearable Electrochemical Lactate Sensing using Osmotic-Capillary Microfluidic Pumping," in *2019 IEEE SENSORS*, 2019, pp. 1-4.

[16] J. Choi, Y. G. Xue, W. Xia, T. R. Ray, J. T. Reeder, A. J. Bandodkar*, et al.*, "Soft, skin-mounted microfluidic systems for measuring secretory fluidic pressures generated at the surface of the skin by eccrine sweat glands," *Lab on a Chip,* vol. 17, pp. 2572-2580, Aug 7 2017.

[17] Z. Yuan, L. Hou, M. Bariya, H. Y. Y. Nyein, L. C. Tai, W. B. Ji*, et al.*, "A multi-modal sweat sensing patch for cross-verification of sweat rate, total ionic charge, and Na+ concentration," *Lab on a Chip,* vol. 19, pp. 3179-3189, Oct 7 2019.

[18] R. Masoodi and K. M. Pillai, "Darcy's Law-Based Model for Wicking in Paper-Like Swelling Porous Media," *Aiche Journal,* vol. 56, pp. 2257-2267, Sep 2010.

[19] B. M. Cummins, R. Chinthapatla, F. S. Ligler, and G. M. Walker, "Time-Dependent Model for Fluid Flow in Porous Materials with Multiple Pore Sizes," *Analytical Chemistry,* vol. 89, pp. 4377-4381, Apr 18 2017.